Assessment of SMAP Passive-Only Soil Moisture Data (Beta Version)

P. O'Neill, Hydrological Sciences, NASA GSFC; S. Chan, A. Colliander, E. Njoku/JPL; R. Bindlish, T. Jackson/USDA

Figure 1

SMAP L2_SM_P (VPOL)   May 25-27, 2015

wet

dry

SMAP SM in m³/m³

0.00 0.05 0.10 0.15 0.20 0.25 0.30 0.35 0.40 0.45 0.50 0.55 0.60 0.65

Figure 2

Soil Moisture Core Site Candidates

Core cal/val sites [●]

Figure 3

SMAP L2SMP Metrics for March 31- October 26, 2015	ubRMSE (m³/m³)			Bias (m³/m³)			Correlation			N
	SCAH	**SCAV**	DCA	SCAH	**SCAV**	DCA	SCAH	**SCAV**	DCA	
Overall Mean Metrics from Core CV sites	0.043	0.038	0.044	-0.040	-0.018	0.008	0.748	0.781	0.719	13
Overall Mean Metrics from Sparse Networks	0.049	0.048	0.060	-0.044	-0.016	0.020	0.655	0.654	0.590	416

Initial validation of SMAP passive-only derived soil moisture (*beta version*) was done using global *in situ* data from core cal/val sites and sparse networks. Core site results from the current baseline retrieval algorithm [SCA-V] meet mission accuracy requirements of an unbiased RMSE < 0.04 m³/m³.

Earth Sciences Division – Hydrospheric and Biospheric Sciences

Name: Peggy O'Neill, Hydrological Sciences, NASA GSFC

Email: Peggy.E.ONeill@nasa.gov;

Phone: 301-614-5773

References:

SMAP L2_SM_P Soil Moisture Data, Beta Version, User Guide: O'Neill, P. E., S. Chan, E. G. Njoku, T. Jackson, and R. Bindlish, 2015. *SMAP L2 Radiometer Half-Orbit 36 km EASE-Grid Soil Moisture, Version 2*. [indicate subset used]. Boulder, Colorado USA. NASA National Snow and Ice Data Center Distributed Active Archive Center. (http://dx.doi.org/10.5067/3Q9102MCFF72)

Updated ATBD: O'Neill, P. E., E. G. Njoku, T. J. Jackson, S. Chan, and R. Bindlish, 2015. *SMAP Algorithm Theoretical Basis Document: Level 2 & 3 Soil Moisture (Passive) Data Products*. SMAP Project, JPL D-66480, Jet Propulsion Laboratory, Pasadena, CA. (https://nsidc.org/data/docs/daac/smap/sp_l2_smp/pdfs/L2_SM_P_ATBD_v7_Sep2015-po-en.pdf.)

L2SMP Beta Assessment Report: Jackson, T., P. O'Neill, E. Njoku, S, Chan, R. Bindlish, A. Colliander, F. Chen, M. Burgin, S. Dunbar, J. Piepmeier, S. Yueh, D. Entekhabi, M. Cosh, T. Caldwell, J. Walker, X. Wu, A. Berg, T. Rowlandson, A. Pacheco, H. McNairn, M. Thibeault, J. Martínez-Fernández, Á. González-Zamora, M. Seyfried, D. Bosch, P. Starks, D. Goodrich, J. Prueger, M. Palecki, E. Small, J. Calvet, W. Crow, and Y. Kerr, November 16, 2015. *Calibration and Validation for the L2/3_SM_P Beta-Release Data Products*, *Version 2*, SMAP Project, JPL D-93981, Jet Propulsion Laboratory, Pasadena, CA. (http://nsidc.org/data/docs/daac/smap/sp_l2_smp/pdfs/SMAP%20L2_SM_P%20Beta-Level%20Assessment%20Report%20FINAL.pdf)

Journal article: Chan, S., R. Bindlish, P. O'Neill, E. Njoku, T. Jackson, A. Colliander, F. Chen, M. Burgin, S. Dunbar, J. Piepmeier, S. Yueh, D. Entekhabi, M. Cosh, T. Caldwell, J. Walker, X. Wu, A. Berg, T. Rowlandson, A. Pacheco, H. McNairn, M. Thibeault, J. Martínez-Fernández, Á. González-Zamora, M. Seyfried, D. Bosch, P. Starks, D. Goodrich, J. Prueger, M. Palecki, E. Small, J. Calvet, W. Crow, and Y. Kerr, "Assessment of the SMAP Level 2 Passive Soil Moisture Product," *IEEE Trans. on Geoscience and Remote Sensing* [submitted Dec. 2015].

Data Sources: NASA's Soil Moisture Active Passive (SMAP) mission launched on January 31, 2015 into a sun-synchronous 6 am/6 pm orbit. SMAP was developed to provide global mapping of high-resolution soil moisture and freeze-thaw state every 2–3 days using an L-band (active) radar and an L-band (passive) radiometer. The SMAP radiometer began acquiring routine data on March 31, 2015 and continues to operate nominally. The radiometer-derived soil moisture product (L2_SM_P) provides soil moisture estimates posted on a 36 km Earth-fixed grid using brightness temperature observations from descending (6 am) passes.

Technical Description of Figures: The SMAP Project released a beta-quality version of the passive-only soil moisture data in September, 2015. **Figure 1** shows an example of a 3-day composite of SMAP L2SMP soil moisture data, showing expected global wet and dry patterns (including flooding in Texas/Oklahoma in May, 2015). In order to assess the quality of these data and to evaluate the performance of several different soil moisture retrieval algorithms, SMAP soil moisture data from March 31 through October 26, 2015 were compared against locally scaled aggregations of *in situ* measurements of soil moisture data from thirteen core cal/val sites in the U.S., Canada, Argentina, Spain, and Australia (shown by red dots in **Figure 2** against a world map of land cover types) and from over 400 stations in sparse networks located in the U.S. (CRN, SCAN, GPS, COSMOS), France (SMOSMania), and Argentina Pampas). Agreements between the SMAP L2SMP data and the *in situ* data sets are reported in unbiased root mean square error (ubRMSE), bias, and time series correlation. Results from **Figure 3** indicate that the Single Channel Algorithm-Vertical Polarization (SCA-V) currently delivers the best performance of the retrieval algorithms examined. The accuracy of the soil moisture retrievals averaged over the core validation sites was an ubRMSE of 0.038 m^3/m^3, which meets the SMAP mission accuracy requirements of an ubRMSE <0.040 m^3/m^3.

Scientific significance, societal relevance, and relationships to future missions: Soil moisture plays a critical role in linking together the Earth's water, energy, and carbon cycles, and is important to a large number of applications with societal benefit. Initial assessments of the SMAP passive-only soil moisture data as reported in the L2SMP Beta Assessment Report indicated that the beta-release L2SMP product is of a sufficient level of maturity and quality that it is approved for distribution to and use by the larger science and application communities. Additional improvements (including optimization of algorithm parameters and upscaling approaches) and methodology expansions (including increasing the number of core sites, model-based intercomparisons, and results from several intensive field campaigns) are anticipated prior to release of the SMAP L2SMP validated data in May, 2016.

Stereo IKONOS is a viable tool for estimating young forest growth

Christopher S.R. Neigh, Jeffrey Masek, Bruce Cook and Ross Nelson, Biospheric Sciences, NASA GSFC
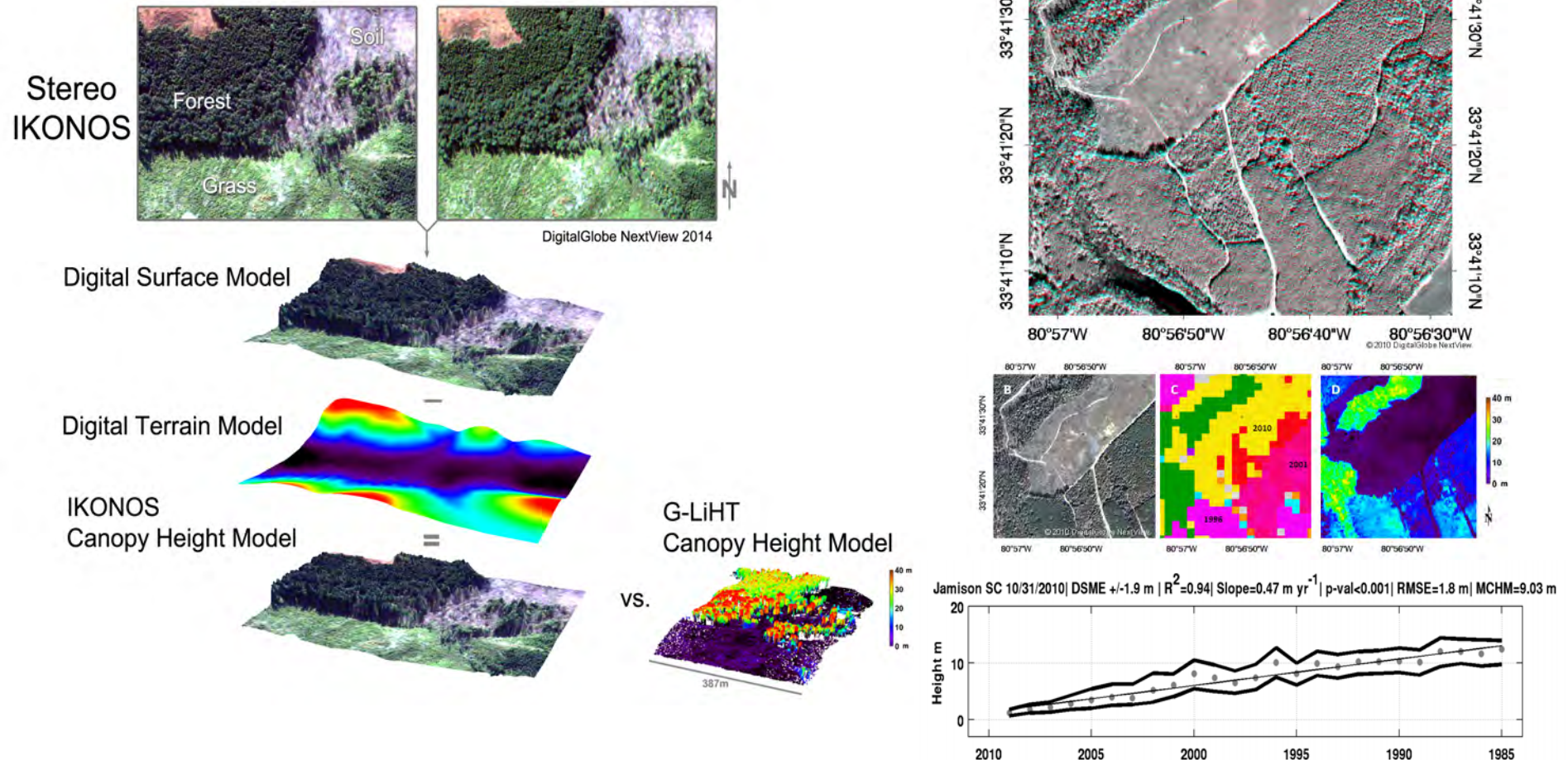
Forest carbon (C) stock is a poorly understood component of the C-cycle. Growth estimates from IKONOS and Landsat are analogous to height and carbon sequestration estimates from field data.

Name: Christopher S. Rudasill-Neigh, Biospheric Sciences, NASA GSFC
E-mail: christopher.s.neigh@nasa.gov
Phone: 301-614-6681

References:

2015 Neigh C.S.R., Masek J., Bourget P., Rishmawi K., Zhao F, Huang C., Cook B., and Nelson R. Regional rates of young US forest growth measured from annual Landsat disturbance history and IKONOS stereo imagery. *Remote Sensing of Environment, in press.*

2014 Neigh C.S.R., Masek J., Bourget P., Cook B., Huang C., Rishmawi K., and Zhao F. Deciphering the precision of stereo IKONOS canopy height models for U.S. forests with G-LiHT airborne LiDAR. *Remote Sensing*, 6 1762-1782. 10.3390/rs6031762

2013 Neigh C.S.R., Masek J., and Nickeson J. High Resolution Satellite Data Open to Government Scientists. *AGU EOS Transactions* 94 (13), 121-123. 10.1002/2013EO130002

Data Sources:
The analysis was performed as part of the North American Forest Dynamics (NAFD) project, a NASA-funded investigation to improve characterization of US forest disturbance patterns in support of the North American Carbon Program (PI: Samuel Goward, University of Maryland; GSFC
CO-I: Jeffrey Masek, Code 618 NASA GSFC). IKONOS imagery were collected from the National Geospatial Intelligence Agency (NGA) under the NextView license agreement with DigitalGlobe and Goddard's LiDAR Hyperspectral and Thermal Imager, (G-LiHT) airborne LiDAR data were collected as part of a the AMIGA-Carb project which is another NASA funded investigation.

Technical Description of Images:

Figure 1. A 3-D graphical description of how canopy height models (CHMs) were created from Stereo IKONOS imagery near Hoquaim WA. True color pan-sharpened IKONOS imagery was subset to show details of forest structure. (top) Left and right within track 1 m resolution stereo IKONOS data were processed calculating image parallax to extract a digital surface model (DSM). (middle) A digital terrain model (DTM) derived from the national elevation (NED) dataset was then subtracted from the DSM to produce CHMs which is an estimate of canopy height with no terrain. We compared CHMs between IKONOS and Goddard's LiDAR Hyperspectral and Thermal Airborne Imager (G-LiHT) which acted as truth.

Figure 2. (A) 3D image of agroforestry (B) IKONOS true color image (C) Landsat disturbance and (D) IKONOS height estimate. © DigitalGlobe NextView 2010 Bottom, forest growth estimate using a *space-for-time* swap of the same location.

Scientific significance:
The spatial distribution of aboveground forest carbon is poorly known over many areas of the globe. Estimates of forest carbon are required for accurate prediction and modeling of changes in carbon sinks and sources. This work is the one of the first to demonstrate that very high-resolution commercial stereo imagery provides highly accurate forest structure in different ecoregions of the US. Combining these data with models one could to infer total aboveground carbon stock and change.

Relevance for future science and relationship to Decadal Survey:
Forest carbon is a critical component of the carbon cycle, and is sensitive to climate change and disturbances. Forest structure observations from very high-resolution commercial instruments are available at no direct cost through NGA's NextView license agreement with DigitalGlobe. Combining these data with Landsat disturbance history, airborne and field measurements, one could provide the necessary data products to infer aboveground carbon stock in forests worldwide. Current work has been extended to study the taiga-tundra transition zone to reduce uncertainties about the distribution of forest cover and establish a baseline extent of the northern forest limit.

Early spring post-fire snow albedo dynamics in high latitude boreal forests using Landsat-8 OLI data

Zhuosen Wang and Miguel O. Román, Terrestrial Information Systems, NASA GSFC
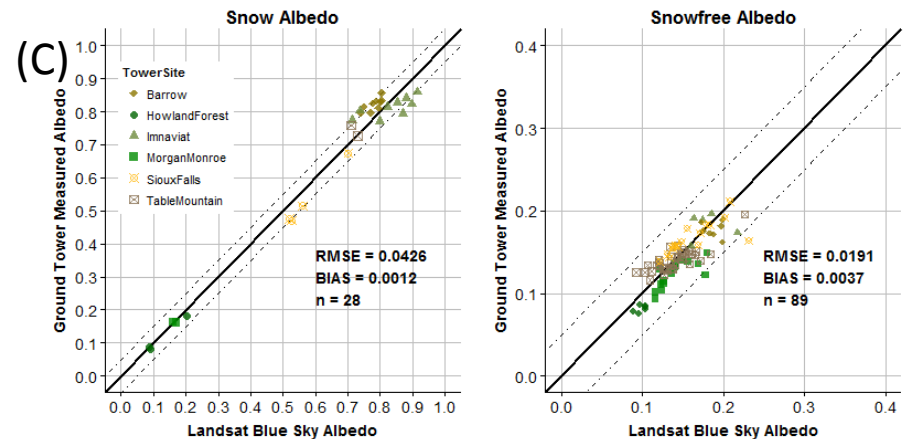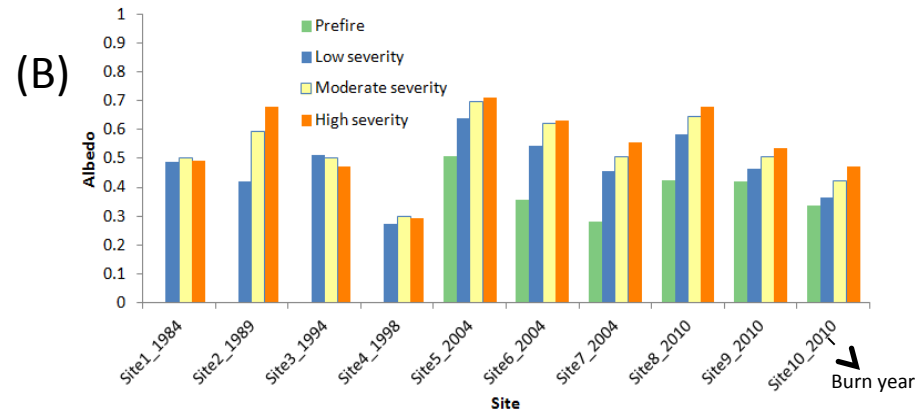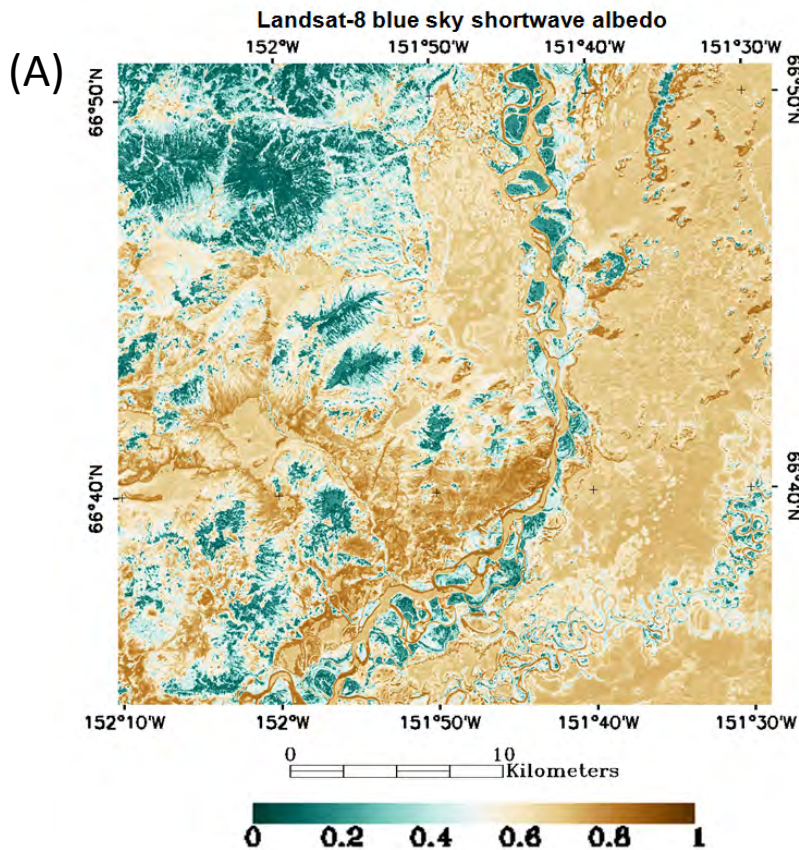
Fine spatial resolution albedo from high quality Landsat-8 data enhances the ability to detect the early spring post-fire albedo dynamics at the landscape scale by considering the significant spatial heterogeneity of burn severity.

Name: Zhuosen Wang, Terrestrial Information Systems, NASA GSFC
E-mail: zhuosen.wang@nasa.gov
Phone: 301-614-5140

References:

Wang, Z., A. M. Erb, C. B. Schaaf, Q. Sun, Y. Liu, Y. Yang, M. O. Román, Y. Shuai, K. A. Casey, 2015: Early spring post-fire snow albedo dynamics in high latitude boreal forests using Landsat-8 OLI data, *Remote Sensing of Environment* (in revision)

Shuai, Y., J. G. Masek, F. Gao, C. B. Schaaf, 2011: An algorithm for the retrieval of 30-m snow-free albedo from Landsat surface reflectance and MODIS BRDF. *Remote Sensing of Environment*, 115(9), 2204–2216. http://doi.org/10.1016/j.rse.2011.04.019

Data Sources: Landsat-8 OLI blue sky shortwave albedo calculated from Landsat-8 OLI surface reflectance and MODIS BRDF/Albedo (MCD43A) products; Burn severity datasets from Monitoring Trends in Burn Severity (MTBS) project; Land cover from The National Land Cover Database (NLCD) products; Ground tower based albedo measurements from the International Baseline Surface Radiation Network (BSRN), NOAA's Surface Radiation Budget Network (SURFRAD), the Arctic Observatory Network (AON) and the Ameriflux network.

Technical Description of Figures:

Graph (A): Landsat-5 TM and Landsat-7 ETM+ signals (8-bit) over snow covered areas without upper canopy cover are commonly saturated. However, the 12-bit Landsat-8 OLI, with a much improved Signal-to-Noise Ratios, allows for the generation of blue sky snow albedo values and improves the analysis of post-fire albedo dynamics at the landscape (< 100m) scale.

Graph (B): Fire and fire severity play an important role in early spring albedo values, which influences snowmelt and localized atmospheric warming. Post fire albedo dynamics within a fire scar are impacted by burn severity.This graph shows the early spring albedo in 2014 over different burn severity at ten burn sites burned from 1984 to 2010. The 2014 early spring albedo values were generally higher in the more recently burned fire scars (2004 and 2010) than in fires that burned prior to 1998. These differences were primarily driven by the vegetation recovery as grasslands were replaced by more shrub and scrub dominated land covers. For sites burned in 2004 or 2010, high severity areas show the highest albedo. Albedo decreased in conjunction with burn severity such that the albedo in moderate and low severity burns exhibited mid-range and low albedo values respectively.

Graph (C): The Landsat-8 blue sky shortwave albedo is evaluated using ground tower based measurements from BSRN, SURFRAD, AON and Ameriflux network. The accuracy of Landsat-8 blue sky shortwave albedo is well within the expected range. The overall RMSE of the combined snow and snow-free data is 0.0267 with a bias of 0.0031 between Landsat-8 blue sky shortwave albedo and ground measurements. Separately, the RMSE and bias for snow scenes were 0.0426 and 0.0012 respectively and for the snow-free scenes was 0.0191 and 0.0037 respectively.

Scientific significance, societal relevance, and relationships to future missions: Since the frequency and severity of wildfires in Arctic and boreal systems is expected to increase in the coming decades, the dynamics of albedo in response to these rapid surface changes will increasingly impact the energy balance and contribute to other climate processes and physical feedback mechanisms. While the importance of post-fire albedo dynamics can be deduced from 500m MODIS albedo product at regional and global scales, our study addresses the particular importance of early spring post-fire albedo dynamics at the landscape scale using 30m Landsat albedo by considering the significant spatial heterogeneity of burn severity, and the impact of snow on the early spring albedo of various vegetation recovery types. This work expands the USGS Landsat albedo product (currently snow-free only) to produce snow albedo which is an important parameter for NASA Arctic-Boreal Vulnerability Experiment (ABoVE) major field campaign..

Earth Sciences Division – Hydrospheric and Biospheric Sciences